

Magnetic and Optical Properties of Novel Lanthanide(III) Complexes Based on Schiff Base and β -Diketonate Ligands

Yufeng Jia,^A Hongfeng Li,^A Peng Chen,^A Ting Gao,^{A,B,C} Wenbin Sun,^A and Pengfei Yan^{A,C}

^AKey Laboratory of Functional Inorganic Material Chemistry (MOE), School of Chemistry and Materials Science, Heilongjiang University, No. 74, Xuefu Road, Nangang District, Harbin 150080, China.

^BKey Laboratory of Chemical Engineering Process and Technology for High-Efficiency Conversion, College of Heilongjiang Province, No. 74, Xuefu Road, Nangang District, Harbin 150080, China.

^CCorresponding authors. Email: gaotingmail@sina.cn; yanpf@vip.sina.com

A series of lanthanide-based self-assembling complexes constructed from Schiff base and β -diketonate ligands have been synthesised by the same method. They are one dimensional complexes ($\{[\text{Ln}(\text{H}_2\text{L})(\text{tta})_2(\text{OAc})]\cdot 0.5\text{H}_2\text{O}\}_n$ (Ln = Eu (**1**), Gd (**2**), Dy (**3**), Yb (**4**); $\text{H}_2\text{L} = N,N'$ -bis(salicylidene)butane-1,4-diamine, $\text{tta} = 2$ -thenoyltrifluoroacetone). Complexes **1** and **4** exhibit characteristic metal-centred emission in the solid state. The lifetimes and quantum yields of luminescence were also determined. Magnetic analysis reveals that complex **3** exhibits field-induced single-molecule magnet (SMM) behaviour with an energy barrier of 24.07 K.

Manuscript received: 2 April 2018.

Manuscript accepted: 11 June 2018.

Published online: 18 July 2018.

Introduction

In the past decade, the study of lanthanide complexes has gained great recognition owing to their fascinating photoluminescence^[1] and magnetism.^[2,3] To date, a large number of lanthanide organic ligands with allowed $\pi-\pi^*$ transitions in the UV region have been synthesised and their excellent characteristics including single-molecule magnets (SMMs)^[4] and fluorescent emission have been extensively studied.^[5] For these lanthanide ions, the $f-f$ Laporte forbidden transition has a very low absorption coefficient. To solve this problem, more organic ligands like Schiff base and β -diketonate chromophores have been used. Previously, various flexible Schiff base ligands were utilised in our group.^[6] Recently we successfully developed a useful synthetic strategy involving both flexible Schiff base and β -diketonate ligands (hexafluoroacetylacetonate) to isolate a series of lanthanide complexes with luminescent properties.^[7] Notably, β -diketonates are ideal candidates as light-harvesting chromophores for sensitisation of visible light and luminescence from Ln^{III} ions.^[8] However, β -diketonate ligands affording a neutral complex cannot protect Ln^{III} ions from solvent molecules which can quench emission.^[9] Therefore, other well designed chromophores should take part in the coordination to form more stable complexes.^[10] Our strategy to obtain luminescent complexes consisted in using flexible Schiff base oxygen donors which can stabilise Ln^{III} centres and transfer energy efficiently to the lanthanide ions, potentially enhancing the luminescent properties. With this in mind, we had chosen the flexible Schiff base (N,N' -bis(salicylidene)butane-1,4-diamine) as a ligand in lanthanide complexes due to

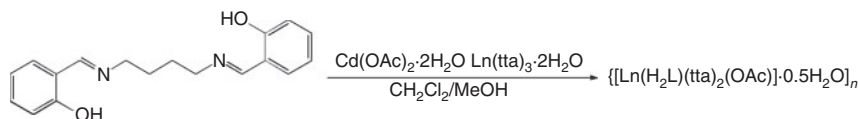
its bridging properties via the O-donor in Ar-OH and its fluorescence properties.^[11-13]

In addition, the single-molecule magnet (SMM) behaviour of 1D spiral chain lanthanide complexes has been the subject of numerous research activities. The Dy^{III} ion has been widely used in the synthesis of molecule-based magnetic materials.^[14-16] The Dy^{III} ion means that 4f metal-based SMMs could possess larger energy barriers, which provide proper orientation of the magnetic principal axes of its ion and reduces quantum tunneling of the magnetisation (QTM).^[17] β -Diketonate ligands have generated increasing interest in the field of SMMs because of a high-order single axis defining the local symmetry and providing a suitable ligand field.^[18-20] Therefore an ancillary β -diketonate ligand with steric hindrance was selected here. Based on these considerations, we described four lanthanide(III) complexes achieved by using a flexible Schiff-base and a β -diketonate ligand, $\{[\text{Ln}(\text{H}_2\text{L})(\text{tta})_2(\text{OAc})]\cdot 0.5\text{H}_2\text{O}\}_n$ (Ln = Eu (**1**), Gd (**2**), Dy (**3**), Yb (**4**); $\text{H}_2\text{L} = N,N'$ -bis(salicylidene)butane-1,4-diamine, $\text{tta} = 2$ -thenoyltrifluoroacetone).

Results and Discussion

Synthesis

The complexes $\{[\text{Ln}(\text{H}_2\text{L})(\text{tta})_2(\text{OAc})]\cdot 0.5\text{H}_2\text{O}\}_n$ (Ln = Eu (**1**), Gd (**2**), Dy (**3**), Yb (**4**)), synthesised by the reaction of H_2L with $\text{Cd}(\text{OAc})_2\cdot 2\text{H}_2\text{O}$ in a 1 : 1 molar ratio in $\text{CH}_2\text{Cl}_2/\text{MeOH}$ produce a yellow clarified liquid (Scheme 1). Yellow crystals suitable for X-ray analysis were obtained by slow diffusion of methanol with $\text{Ln}(\text{tta})_3\cdot 2\text{H}_2\text{O}$ into the yellow solution for one week.



Scheme 1. Schematic representation of complexes **1–4**.

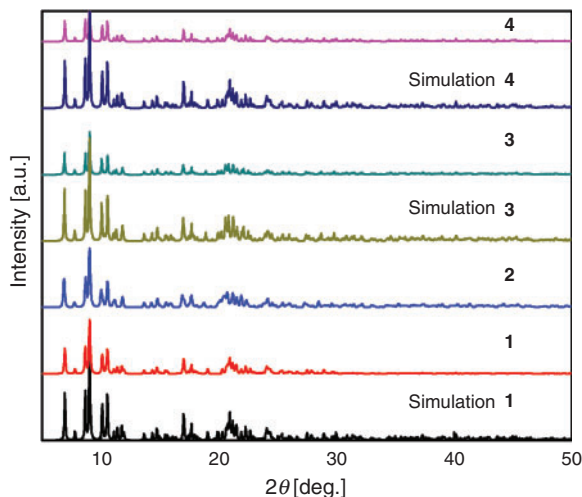


Fig. 1. PXRD patterns for **1–4**.

IR Spectra

The IR absorption spectra of the ligand and complexes **1–4** are shown in Fig. S1 (Supplementary Material). Taking **1** as an example, the broad but weak O–H stretching vibration of the free H_2L ligand at $\sim 2855\text{ cm}^{-1}$ is replaced by a band at $\sim 3695\text{ cm}^{-1}$ in complex **1** due to the N–H vibration in $C=N^+-H$. This band indicates that the hydrogen atoms are still involved in intramolecular H-bonding with the phenolic oxygen. The C=N stretching vibration in complex **1** shifts to a higher wavenumber (by $20\text{--}30\text{ cm}^{-1}$ to $\sim 1657\text{ cm}^{-1}$).^[21]

X-Ray crystallographic analysis has revealed that complexes **1–4** are isomorphous, as revealed by comparison of their powder X-ray diffraction (PXRD) patterns (Fig. 1). The PXRD patterns of complexes **1–4** are in agreement with the simulated ones from the respective single-crystal X-ray data. Taking **1** as an example, the unit cell of complex **1** crystallises in the monoclinic space group $P2_1/n$. The perspective view of the molecular structure of **1** was shown as a dodecahedron^[22] in Fig. 2b. Crystallographic details are provided in Table 1 and selected bond lengths of the coordination environment of the metal centres are listed in Table S1 (Supplementary Material). The organic ligand H_2L is involved in linking the one dimensional chain structure. As a result, each H_2L acts a bridge between two Eu^{III} atoms. Cd^{2+} ions are not observed in the structure. The unique Eu^{III} ions are eight-coordinated by two different H_2L anionic oxygen atoms, two oxygen atoms from an acetate anion, and four oxygen atoms from two tta ligands. The $Eu-O$ (tta) distances range from 2.395 (3) to 2.409(3) Å. Notably, the $Eu-O$ bond distances for H_2L atoms O4 and O8 of the ligands (2.293(2) and 2.310(2)) are shorter than those oxygen atoms of acetate (2.461(3) and 2.484 (2)). The oxygen atoms (O6, O7) of the acetate group chelate the europium ion. One Schiff base ligand displays a curved configuration in which the backbone oxygen atoms (O4, O15) link $Eu1$ and $Eu2$ ions. The $O4-Eu-O8$ angle is 158.69° . The hydrogen atoms located on the two nitrogen atoms are involved in

intramolecular hydrogen bonding with the deprotonated phenol oxygen atoms, thus indicating that a proton migration occurs in the complexation reactions.

Luminescence Properties

The UV-vis absorption data of complexes **1–4**, $Eu(tta)_2 \cdot 2H_2O$, and H_2L are presented in Fig. S2 (Supplementary Material). In MeOH, H_2L consists of three main absorptions at ~ 215 , 255, 315 nm which are assigned to the $\pi-\pi^*$ transitions of Ar-OH and the imine group. As for **1**, there are three sets of absorption bands at ~ 237 , 270, and 346 nm, which are due to the intra-ligand transitions of the ligand. The emission spectra of complex **1** in the solid state tested at room-temperature are presented in Fig. 3. Based on a maximum excitation at 368 nm in the solid state, the emission spectrum of Eu^{III} is observed at 614 nm with a strong and unique emission peak. Four typical emission bands of the Eu^{III} ion are observed, 590 (${}^5D_0 \rightarrow {}^7F_0$), 614 (${}^5D_0 \rightarrow {}^7F_2$), 650 (${}^5D_0 \rightarrow {}^7F_3$), and 696 nm (${}^5D_0 \rightarrow {}^7F_4$). The free H_2L ligand does not exhibit luminescence under similar conditions. The H_2L provides efficient energy transfer for the sensitisation of the Ln^{3+} ion. The lifetime of **1** is 417.19 μs in the solid state.

NIR Luminescence

The NIR emission spectra of complex **4** in the solid state tested at room temperature are presented in Fig. 4. Excited at 380 nm with maximum excitation, the typical NIR emission band of Yb^{III} centred at 980 nm was observed, which is assigned to the ${}^2F_{5/2} \rightarrow {}^2F_{7/2}$ transition. Two other broad bands centred at 993 and 1028 nm are also observed. The free H_2L ligand does not exhibit NIR luminescence under the same conditions. The H_2L provides efficient energy transfer for the sensitisation of the Yb^{3+} ion. The lifetime of **4** was $\tau_1 = 9681.93\text{ ns}$ in the solid state.

In general, the widely accepted energy transfer mechanism of the luminescent lanthanide complexes is proposed by Crosby.^[23] In order to make the energy transfer effective, the energy-level match between the lowest triplet energy level (T_1) of the ligand and the lowest excited state level of the Ln^{III} ion becomes one of the most important factors dominating the luminescence properties of the complexes. On account of the difficulty in observing the phosphorescence spectrum of the ligand, the emission spectrum of the complex $\{[Gd(H_2L)(tta)_2(OAc)] \cdot 0.5H_2O\}_n$ (**2**) at 77 K is used to estimate the triplet state energy level of the ligand. The singlet state energy level of H_2L is estimated by referring its absorbance edge, which is 24814 cm^{-1} (403 nm). The triplet (T_1) energy levels are calculated by referring to the lower wavelength emission peaks of the corresponding phosphorescence spectrum of the Gd^{III} complex, which are 20325 cm^{-1} (492 nm) (Fig. S3, Supplementary Material). It is known that the gap $\Delta E(T_1-Ln^{III})$ should be intermediate for maximum energy transfer, otherwise too large or too small a gap would decrease the efficiency of energy transfer. According to Latva et al.,^[24] the ligand-to-metal transfer process could occur effectively when the energy gap is in the region of $2500\text{--}3200\text{ cm}^{-1}$. Therefore, the energy gaps between the triplet state of H_2L and the resonance energy level of Eu^{III} was

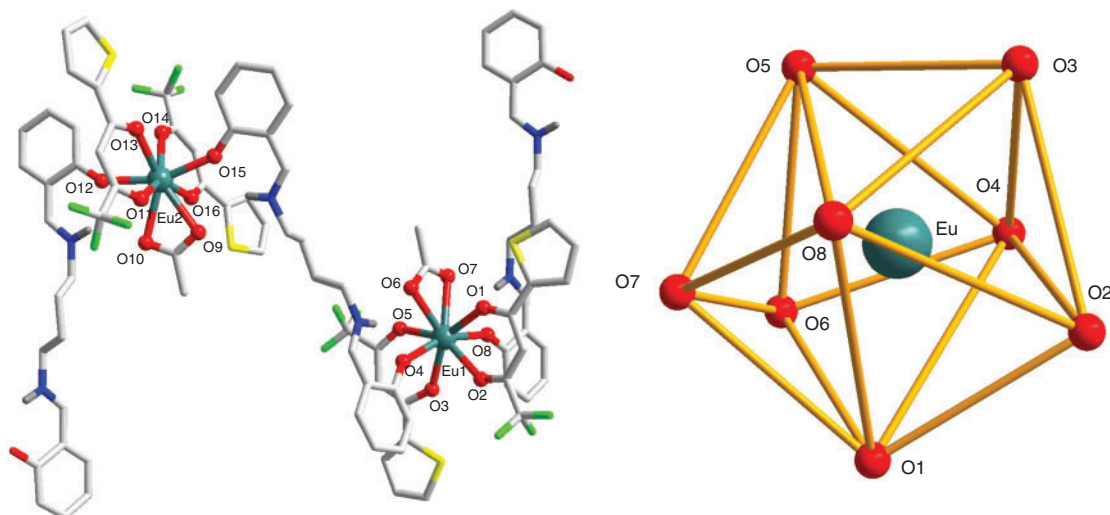


Fig. 2. (a) Crystal structure of **1**; hydrogen atoms are omitted for clarity. Colour code: dark green (Eu), blue (N), red (O), grey (C), yellow (S), green (F). Selected bond length (Å) and bond angles (°): Eu(1)–O(4) 2.293(2), Eu(1)–O(1) 2.395(3), Eu(1)–O(8) 2.310(2), Eu(1)–O(3) 2.402(2), Eu(1)–O(2) 2.401(3), Eu(1)–O(5) 2.409(3), Eu(1)–O(6) 2.461(3), Eu(1)–O(7) 2.484(2); O4–Eu–O8 158.69. (b) Perspective view of the coordination polyhedron for the Eu^{3+} ions in **1**.

Table 1. Emission data for complexes **1** and **4**

Complex	Medium	λ_{ex} [nm]	λ_{em} [nm]	τ_{em}	Transition type
1	Solid	368	614	417.19 μs	590 ($^5\text{D}_0 \rightarrow ^7\text{F}_0$), 614 ($^5\text{D}_0 \rightarrow ^7\text{F}_2$), 650 ($^5\text{D}_0 \rightarrow ^7\text{F}_3$), 696 nm ($^5\text{D}_0 \rightarrow ^7\text{F}_4$)
4	Solid	380	980	9681.93 ns	980, 993, 1028 nm ($^2\text{F}_{5/2} \rightarrow ^2\text{F}_{7/2}$)

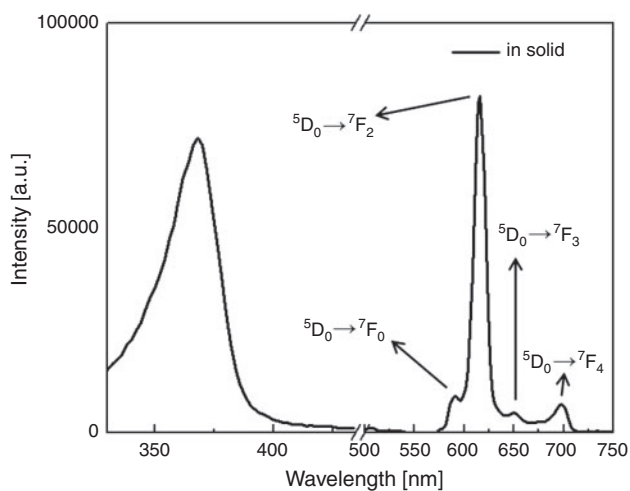


Fig. 3. Luminescence excitation and emission spectra of **1** in the solid state at room temperature.

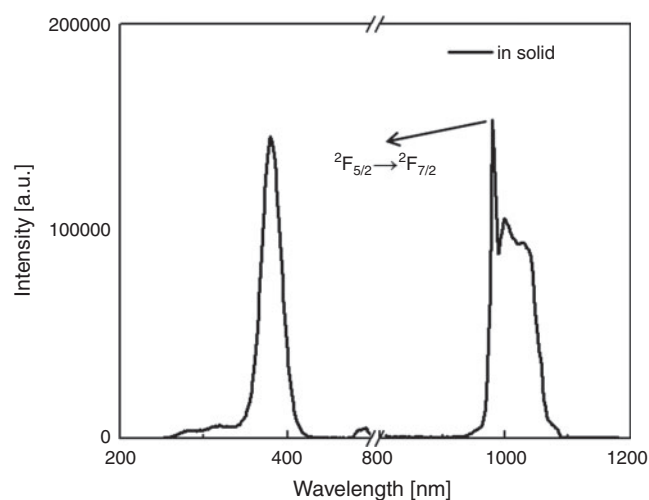


Fig. 4. NIR luminescence excitation and emission spectra of **4** in the solid state at room temperature.

calculated (Fig. 5). The energy gap, $\Delta E(T_1 - ^5\text{D}_0)$, is 2825 cm^{-1} for **1**. The T_1 energy level of H_2L is thus 10025 cm^{-1} higher than the $^2\text{F}_{2/5}$ level of Yb^{III} (10300 cm^{-1}). Therefore, it is easy to understand that energy transfer from the ligand to Eu^{III} .

Magnetic Susceptibility Studies

Direct current (dc) magnetic susceptibility studies of **3** have been carried out in an applied magnetic field of 2000 Oe (Fig. 6)

in the temperature range 300–2 K. The $\chi_{\text{m}}T$ value of **3** at 300 K is $13.83 \text{ cm}^3 \text{ K mol}^{-1}$, which is very close to the value of $14.17 \text{ cm}^3 \text{ K mol}^{-1}$ for one uncoupled Dy^{III} ion. It is also obvious that the $\chi_{\text{m}}T$ product steadily declines with the lowering of temperature and exhibits a rapid increase in the magnetisation at low field. The maximum of magnetisation is 4.68 in the range of 300–100 K and then further decreases dramatically to reach a minimum of $11.15 \text{ cm}^3 \text{ K mol}^{-1}$ at 2 K. These thermal behaviours are

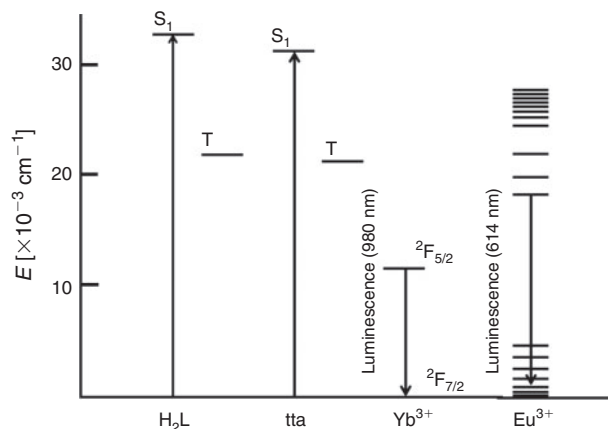


Fig. 5. Schematic energy level diagram and energy transfer processes for complexes **1** and **4**. S_1 , first excited singlet state; T, first excited triplet state

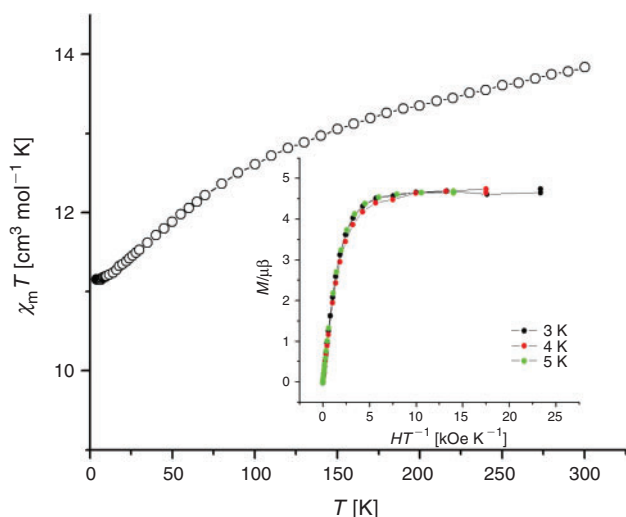


Fig. 6. Temperature dependence of $\chi_m T$ at 2000 Oe for complex **3**; inset: M versus HT^{-1} plot at 3, 4, and 5 K.

mostly due to the progressive depopulation of the excited Stark sublevels of Dy^{III} and possible weak antiferromagnetic interactions between molecules. The magnetisation of complex **3** at 3, 4, and 5 K is shown in the inset of Fig. 6 which exhibits a rapid increase in the magnetisation at low field. The maximum of magnetisation is $4.74 \mu_{\text{B}}$, which is lower than the expected saturation value of $10 \mu_{\text{B}}$ for one Dy^{III} ion ($10 \mu_{\text{B}}$ for each Dy^{III} ion), likely due to the low-lying excited states and the important crystal-field effect at the Dy^{III} ion that eliminates the 16-fold degeneracy of the $^6H_{15/2}$ ground state.^[25] The temperature and frequency dependencies of the alternating current (ac) susceptibilities have been measured under zero-dc field for **3**. As given in Fig. 7, it shows temperature and frequency dependence, which reveals the typical features associated with the SMM behaviour. On cooling, χ' and χ'' increase again below 4 K, and this indicates the onset of pure quantum tunnelling. Moreover, it is also noteworthy that the temperature dependence of out-of-phase ac susceptibility does not go to zero below 4 K, as for most SMMs, which might be indicative of a fast relaxation process that becomes dominant in the lower temperature region. The magnetisation relaxation time (τ) is derived from the frequency dependence of the ac susceptibility between 2 and 6 K

and the Arrhenius plot obtained from these data is given in Fig. 8. The energy barrier is $U_{\text{eff}} = 24.07(0.57)$ K with a pre-exponential factor (τ_0) of $\sim 5.5 \times 10^{-6}$ s based on the Arrhenius law [$\tau = \tau_0 \exp(U_{\text{eff}}/kT)$], which is consistent with the expected τ_0 of 10^{-6} – 10^{-11} for SMMs.

Conclusions

To summarise, through the rational choice of H_2L and a strong electron-withdrawing ligand, namely thenoyltrifluoroacetate (tta), four lanthanide complexes $\{[\text{Ln}(\text{H}_2\text{L})(\text{tta})_2(\text{OAc})] \cdot 0.5\text{H}_2\text{O}\}_n$ ($\text{Ln} = \text{Eu}$ (**1**), Gd (**2**), Dy (**3**), Yb (**4**)) have been successfully synthesised. Complexes **1** and **4** show visible luminescence and NIR luminescence properties with the strong and unique emission of Eu^{III} and Yb^{III} respectively. Magnetic analysis reveals that the Dy^{III} ions dominate the antiferromagnetic properties of complex **3**, which features SMM behaviour.

Experimental

General Methods

All chemicals except $\text{Ln}(\text{tta})_3 \cdot 2\text{H}_2\text{O}$ ($\text{Ln} = \text{Eu}$ (**1**), Gd (**2**), Dy (**3**), Yb (**4**)) and H_2L were obtained from commercial sources and used without further purification. $\text{Ln}(\text{tta})_3 \cdot 2\text{H}_2\text{O}$ was prepared by the reactions of tta and the lanthanide metal chloride. The lanthanide precursors $\text{Ln}(\text{tta})_3 \cdot 2\text{H}_2\text{O}$ ($\text{Ln} = \text{Eu}$ (**1**), Gd (**2**), Dy (**3**), Yb (**4**)) were synthesised according to the literature.^[26] H_2L was obtained by condensation of 1,4-diaminobutane and salicylaldehyde in a 1 : 2 molar ratio in absolute methanol according to previously reported synthetic methods.^[27] Elemental analyses (C, H, N) were performed using a Perkin–Elmer 2400 analyser. IR spectra were obtained using a Perkin–Elmer 60000 spectrophotometer. UV spectra were recorded with a Shimadzu UV2240 spectrophotometer. Fluorescence spectra of the complexes were recorded using a FLSP920 spectrophotometer equipped with a xenon lamp and a quartz carrier at room temperature. Luminescence lifetimes were recorded using a single photon counting spectrometer with a microsecond pulse lamp as the excitation source. The overall quantum yields of both europium and ytterbium complexes were measured in MeOH ($\sim 10^{-5}$ mol L^{-1}) at room temperature and referenced to a water solution of $\text{Ru}(\text{bpy})_3\text{Cl}_2$ ($\text{bpy} = 2,2'$ -bipyridine, $\phi = 0.028$), and through the following expression:

$$\phi_{\text{overall}} = \frac{n^2 A_{\text{ref}} I}{n_{\text{ref}}^2 A I_{\text{ref}}} \phi_{\text{ref}} \quad (1)$$

In Eqn 1, n , I , and A denote the refractive index of the solvent, the area of the emission spectrum, and the absorbance at the excitation wavelength, respectively, and ϕ_{ref} represents the quantum yield of the standard $\text{Ru}(\text{bpy})_3\text{Cl}_2$ solution. The quantum yields of complexes **1** and **4** in methanol solutions are estimated by the equation $\phi_{\text{Ln}} = \tau_{\text{obs}}/\tau_0$. The magnetic susceptibility for complex **3** was measured with a Quantum Design MPMS XL-7 SQUID-VSM magnetometer. The magnetic corrections were made by using Pascal's constants.

Syntheses of Complexes 1–4

Synthesis of Complex $\{[\text{Eu}(\text{H}_2\text{L})(\text{tta})_2(\text{OAc})] \cdot 0.5\text{H}_2\text{O}\}_n$ (**1**)

These complexes were prepared by an identical method. The synthesis of complex **1** is described herein. A methanol solution (20 mL) of $\text{Cd}(\text{OAc})_2 \cdot 2\text{H}_2\text{O}$ (0.266 g, 1 mmol) was added to a solution of H_2L (0.296 g, 1 mmol) in 16 mL of dichloromethane.

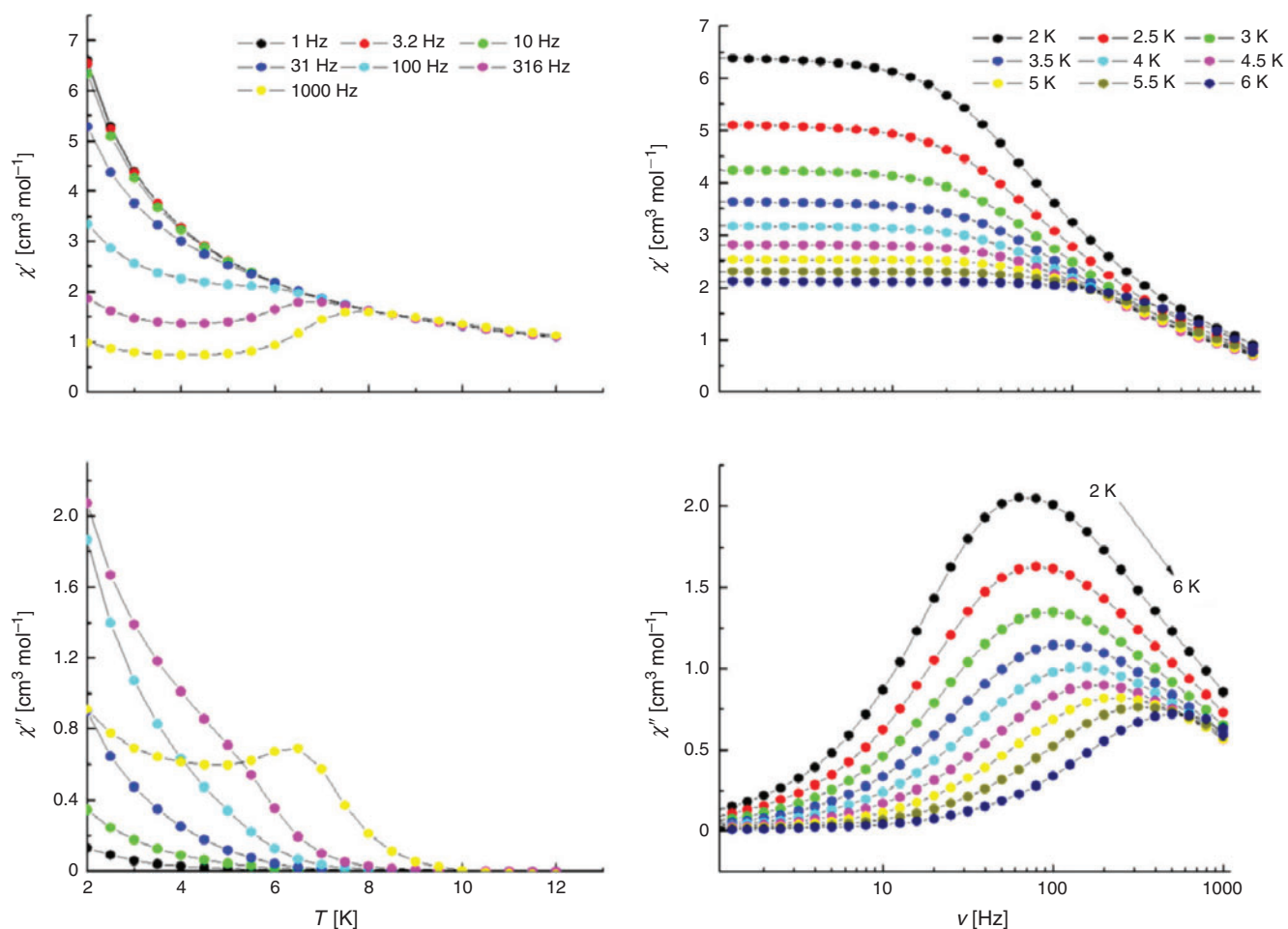


Fig. 7. (Left) Temperature dependence of the in-phase (χ') and out-of-phase (χ'') ac susceptibility of complex **3** under 0 Oe in the frequency range 1–1000 Hz at 2–12 K. (Right) Frequency dependence of the in-phase and out-of-phase ac susceptibilities under 0 Oe in the temperature range 2–6 K for **3**.

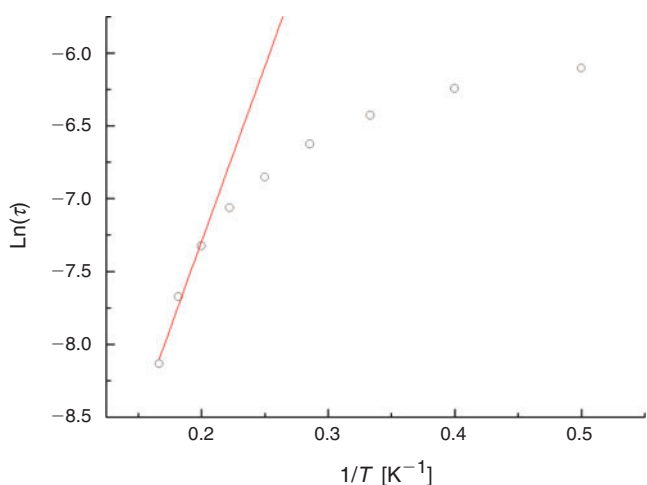


Fig. 8. Magnetisation relaxation time, $\ln\tau$, versus T^{-1} plot for complex **3** under zero-dc field. The solid line is fitted with the Arrhenius law.

After refluxing for 1 h, the solution changed to yellow. The mixture was filtered and the precipitate was removed from the solution. The filtrate was diffused slowly by a methanol solution (16 mL) of $\text{Eu}(\text{tta})_3 \cdot 2\text{H}_2\text{O}$ (0.218 g, 0.25 mmol) and allowed to stand undisturbed at room temperature for one week. Yellow crystals of **1** were obtained in 51 % yield (0.121 g). Anal. Calc.

for $\text{C}_{36}\text{H}_{32}\text{EuF}_6\text{N}_2\text{O}_{8.5}\text{S}_2$: C 45.10, H 3.36, N 2.92. Found: C 45.46, H 3.34, N 2.93 %. ν_{max} (KBr pellet)/ cm^{-1} 3695 (m), 2900 (w), 1657 (m), 1599 (s), 1530 (s), 1480 (w), 1345 (w), 1300 (s), 1198 (s), 1134 (s), 1018 (w), 934 (m), 859 (w), 775 (m), 677 (w), 635 (w), 577 (s). λ_{max} (MeOH)/nm 237, 270, 346.

Synthesis of Complex $\{[\text{Gd}(\text{H}_2\text{L})(\text{tta})_2(\text{OAc})] \cdot 0.5\text{H}_2\text{O}\}_n$ (**2**)

The title compound was obtained in 52 % yield (0.124 g). Anal. Calc. for $\text{C}_{36}\text{H}_{32}\text{GdF}_6\text{N}_2\text{O}_{8.5}\text{S}_2$: C 44.85, H 3.35, N 2.90. Found: C 45.20, H 3.35, N 2.90 %. ν_{max} (KBr pellet)/ cm^{-1} 3706 (m), 2889 (w), 1657 (m), 1608 (s), 1540 (s), 1478(w), 1342(w), 1300(s), 1196(s), 1134(s), 1020(w), 936(m), 860(w), 778(m), 675(w), 639(w), 580(s). λ_{max} (MeOH)/nm 237, 270, 346.

Synthesis of Complex $\{[\text{Dy}(\text{H}_2\text{L})(\text{tta})_2(\text{OAc})] \cdot 0.5\text{H}_2\text{O}\}_n$ (**3**)

The title compound was obtained in 56 % yield (0.135 g). Anal. Calc. for $\text{C}_{36}\text{H}_{32}\text{DyF}_6\text{N}_2\text{O}_{8.5}\text{S}_2$: C 44.61, H 3.33, N 2.89. Found: C 44.95, H 3.32, N 2.90 %. ν_{max} (KBr pellet)/ cm^{-1} 3696 (m), 2900 (w), 1657 (m), 1599 (s), 1530 (s), 1480 (w), 1345 (w), 1300 (s), 1193 (s), 1130 (s), 1018 (w), 901 (m), 850 (w), 775 (m), 677 (w), 635 (w), 577 (s). λ_{max} (MeOH)/nm 237, 270, 346.

Synthesis of Complex $\{[\text{Yb}(\text{H}_2\text{L})(\text{tta})_2(\text{OAc})] \cdot 0.5\text{H}_2\text{O}\}_n$ (**4**)

The title compound was obtained in 51 % yield (0.124 g). Anal. Calc. for $\text{C}_{36}\text{H}_{32}\text{YbF}_6\text{N}_2\text{O}_{8.5}\text{S}_2$: C 44.13, H 3.29, N 2.86.

Table 2. Crystal data and structure refinement for complexes 1, 3, and 4

Crystal data	1	3	4
CCDC	182973	1829726	1829733
Empirical formula	C ₃₆ H ₃₁ EuF ₆ N ₂ O _{8.5} S ₂	C ₃₆ H ₃₂ DyF ₆ N ₂ O _{8.5} S ₂	C ₃₆ H ₃₂ YbF ₆ N ₂ O _{8.5} S ₂
Formula weight	958.72	969.25	979.80
Temperature [K]	293.0	293.0	293.0
Wavelength [Å]	0.71073	0.71073	0.71073
Crystal system	monoclinic	monoclinic	monoclinic
Space group	<i>P</i> 2 ₁ / <i>n</i>	<i>P</i> 2 ₁ / <i>n</i>	<i>P</i> 2 ₁ / <i>n</i>
<i>a</i> [Å]	12.3916(3)	12.4200(5)	12.4294(3)
<i>b</i> [Å]	19.0680(4)	19.1407(7)	19.2491(7)
<i>c</i> [Å]	18.0104(4)	17.7758(7)	17.5665(6)
α [deg.]	90.00	90.00	90.00
β [deg.]	105.576(2)	105.535(5)	105.597(3)
γ [deg.]	90.00	90.00	90.00
<i>V</i> [Å ³]	4099.27(16)	4071.4(3)	4048.1(2)
<i>Z</i>	4	4	4
Calculated density [Mg m ⁻³]	1.553	1.581	1.608
μ [mm ⁻¹]	1.710	2.016	2.492
F(000)	1916.0	1928.0	1944.0
θ range	6.304 to 52.744	6.302 to 52.74	6.302 to 52.744
Limiting indices	$-15 \leq h \leq 13$, $-17 \leq k \leq 23$, $-11 \leq l \leq 22$	$-15 \leq h \leq 15$, $-23 \leq k \leq 17$, $-22 \leq l \leq 21$	$-15 \leq h \leq 15$, $-24 \leq k \leq 10$, $-21 \leq l \leq 21$
Reflections collected	17603	18903	17478
Completeness to $\theta = 27.5^\circ$	100%	100%	100%
Data/restraints/parameters	8375/4/496	8318/4/496	8221/1/496
Goodness of fit on F^2	1.014	1.052	1.028
Final <i>R</i> indices [$I > 2\sigma(I)$]	$R_1 = 0.0330$, $wR_2 = 0.0759$	$R_1 = 0.0381$, $wR_2 = 0.0845$	$R_1 = 0.0603$, $wR_2 = 0.1045$
<i>R</i> indices (all data)	$R_1 = 0.0520$, $wR_2 = 0.0834$	$R_1 = 0.0594$, $wR_2 = 0.0966$	$R_1 = 0.0976$, $wR_2 = 0.1179$

Found: C 44.46, H 3.30, N 2.85%. ν_{\max} (KBr pellet)/cm⁻¹ 3696 (m), 2920 (w), 1650 (m), 1608 (s), 1540 (s), 1489 (w), 1349 (w), 1309 (s), 1205 (s), 1141 (s), 1025 (w), 943 (m), 869 (w), 780 (m), 685 (w), 646 (w), 584 (s). λ_{\max} (MeOH)/nm 237, 270, 346.

X-Ray Crystallography

The crystallographic details for **1**, **3**, and **4** are given in Table 2. Diffraction intensity data for single crystals of complexes were collected using a Rigaku R-Axis RAPID imaging-plate X-ray diffractometer at 293 K. The structures were solved by direct methods and refined by full matrix least-squares on F^2 using SHELXTL-97.^[28,29] All non-hydrogen atoms were refined with anisotropic displacement parameters. The unit cell contained a hydrate molecule which had been treated as a diffuse contribution to the overall scattering without specific atom positions by SQUEEZE/PLATON.^[30]

Crystallographic Data

CCDC 182973, 1829726, 1829733 contain the supplementary crystallographic data for **1**, **3**, and **4**. These data can be obtained free of charge from The Cambridge Crystallographic Data Centre via <http://www.ccdc.cam.ac.uk/conts/retreving.html>.

Supplementary Material

The infrared spectra, UV spectra, and visible emission spectra for complexes **1** and **4** are available on the Journal's website.

Conflicts of Interest

The authors declare no conflicts of interest.

Acknowledgements

This work is financially supported by the National Natural Science Foundation of China (nos. 21302045, 51773054 and 51472076).

References

- [1] T. Gao, P. F. Yan, G. M. Li, G. F. Hou, J. S. Gao, *Inorg. Chim. Acta* **2008**, *361*, 2051. doi:10.1016/J.ICA.2007.10.021
- [2] P. F. Yan, P. H. Lin, F. Habib, T. Aharen, M. Murugesu, Z. P. Deng, G. M. Li, W. B. Sun, *Inorg. Chem.* **2011**, *50*, 7059. doi:10.1021/IC200566Y
- [3] P. H. Lin, W. B. Sun, M. F. Yu, G. M. Li, P. F. Yan, M. Murugesu, *Chem. Commun.* **2011**, *47*, 10993. doi:10.1039/C1CC14223B
- [4] Y. Y. Zhu, X. Guo, C. Cui, B. W. Wang, Z. M. Wang, S. Gao, *Chem. Commun.* **2011**, *47*, 8049. doi:10.1039/C1CC12831K
- [5] H. S. Ke, G. F. Xu, Y. N. Guo, P. Gamez, C. M. Beavers, S. J. Teat, J. K. Tang, *Chem. Commun.* **2010**, *46*, 6057. doi:10.1039/C0CC01067G
- [6] O. Sun, T. Gao, J. W. Sun, G. M. Li, H. F. Li, H. Xu, C. Wang, P. F. Yan, *CrystEngComm* **2014**, *16*, 10460. doi:10.1039/C4CE01556H
- [7] X. Hu, W. Dou, C. Xu, X. Tang, J. Zheng, W. Liu, *Dalton Trans.* **2011**, *40*, 3412. doi:10.1039/C0DT01350A
- [8] D. P. Li, X. P. Zhang, T. W. Wang, B. B. Ma, C. H. Li, Y. Z. Li, X. Z. You, *Chem. Commun.* **2011**, *47*, 6867. doi:10.1039/C1CC11659B
- [9] C. Benelli, D. Gatteschi, *Chem. Rev.* **2002**, *102*, 2369. doi:10.1021/CR010303R
- [10] D. R. van Staveren, G. A. V. Albada, J. G. Haasnoot, H. Kooijman, A. M. M. Lanfredi, P. J. Nieuwenhuizen, A. L. Spek, F. Ugozzoli, T. Weyhermüller, J. Reedijk, *Inorg. Chim. Acta* **2001**, *315*, 163. doi:10.1016/S0020-1693(01)00334-6

- [11] X. P. Yang, R. A. Jones, M. M. Oye, A. L. Holmes, W. K. Wong, *Cryst. Growth Des.* **2006**, *6*, 2122. doi:10.1021/CG0603319
- [12] S. Liao, X. P. Yang, R. A. Jones, *Cryst. Growth Des.* **2012**, *12*, 970. doi:10.1021/CG201444P
- [13] X. P. Yang, R. A. Jones, *J. Am. Chem. Soc.* **2005**, *127*, 7686. doi:10.1021/JA051292C
- [14] Y. N. Guo, G. F. Xu, W. Wernsdorfer, L. Ungur, Y. Guo, J. K. Tang, H. J. Zhang, L. F. Chibotaru, A. K. Powell, *J. Am. Chem. Soc.* **2011**, *133*, 11948. doi:10.1021/JA205035G
- [15] J. Long, F. Habib, P. H. Lin, I. Korobkov, G. Enright, L. Ungur, W. Wernsdorfer, L. F. Chibotaru, M. Murugesu, *J. Am. Chem. Soc.* **2011**, *133*, 5319. doi:10.1021/JA109706Y
- [16] F. Habib, P. H. Lin, J. Long, I. Korobkov, W. Wernsdorfer, M. Murugesu, *J. Am. Chem. Soc.* **2011**, *133*, 8830. doi:10.1021/JA2017009
- [17] C. Benelli, D. Gatteschi, *Chem. Rev.* **2002**, *102*, 2369. doi:10.1021/CR010303R
- [18] S. D. Jiang, B. W. Wang, G. Su, Z. M. Wang, S. Gao, *Angew. Chem. Int. Ed.* **2010**, *49*, 7448. doi:10.1002/ANIE.201004027
- [19] N. F. Chilton, S. K. Langley, B. Moubaraki, A. Soncini, S. R. Batten, K. S. Murray, *Chem. Sci.* **2013**, *4*, 1719. doi:10.1039/C3SC22300K
- [20] D. P. Li, X. P. Zhang, T. W. Wang, B. B. Ma, C. H. Li, Y. Z. Li, X. Z. You, *Chem. Commun.* **2011**, *47*, 6867. doi:10.1039/C1CC11659B
- [21] K. Binnemans, Y. G. Galyametdinov, R. V. Deun, D. W. Bruce, S. R. Collinson, A. P. Polishchuk, I. Bikchantaev, W. Haase, A. V. Prosvirin, L. Tinchurina, I. Litvinov, A. Gubajdullin, A. Rakhmatullin, K. Uytterhoeven, L. V. Meervelt, *J. Am. Chem. Soc.* **2000**, *122*, 4335. doi:10.1021/JA993351Q
- [22] S. L. Yang, R. R. Wang, X. J. Jin, C. X. Zhang, Q. L. Wang, *Polyhedron* **2018**, *144*, 101. doi:10.1016/J.POLY.2017.12.030
- [23] G. A. Crosby, R. E. Whan, J. J. Freeman, *J. Phys. Chem.* **1962**, *66*, 2493. doi:10.1021/J100818A041
- [24] M. Latva, H. Takalo, V. M. Mikkala, C. Matachescu, J. C. Rodriguez-Ubis, J. Kankare, *J. Lumin.* **1997**, *75*, 149. doi:10.1016/S0022-2313(97)00113-0
- [25] S. Osa, T. Kido, N. Matsumoto, N. Re, A. Pochaba, J. Mrozinski, *J. Am. Chem. Soc.* **2004**, *126*, 420. doi:10.1021/JA037365E
- [26] A. Lennartson, M. Vestergren, M. Hakansson, *Chem. - Eur. J.* **2005**, *11*, 1757. doi:10.1002/CHEM.200401019
- [27] F. Lam, J. X. Xu, K. S. Chan, *J. Org. Chem.* **1996**, *61*, 8414. doi:10.1021/JO961020F
- [28] O. V. Dolomanov, L. J. Bourhis, R. J. Gildea, J. A. K. Howard, H. Puschmann, *J. Appl. Cryst.* **2009**, *42*, 339. doi:10.1107/S0021889808042726
- [29] G. M. Sheldrick, *Acta Crystallogr. Sect. C* **2015**, *71*, 3. doi:10.1107/S2053229614024218
- [30] A. L. Speck, *Acta Crystallogr. Sect. C* **2015**, *C71*, 9. doi:DOI:10.1107/S2053229614024929